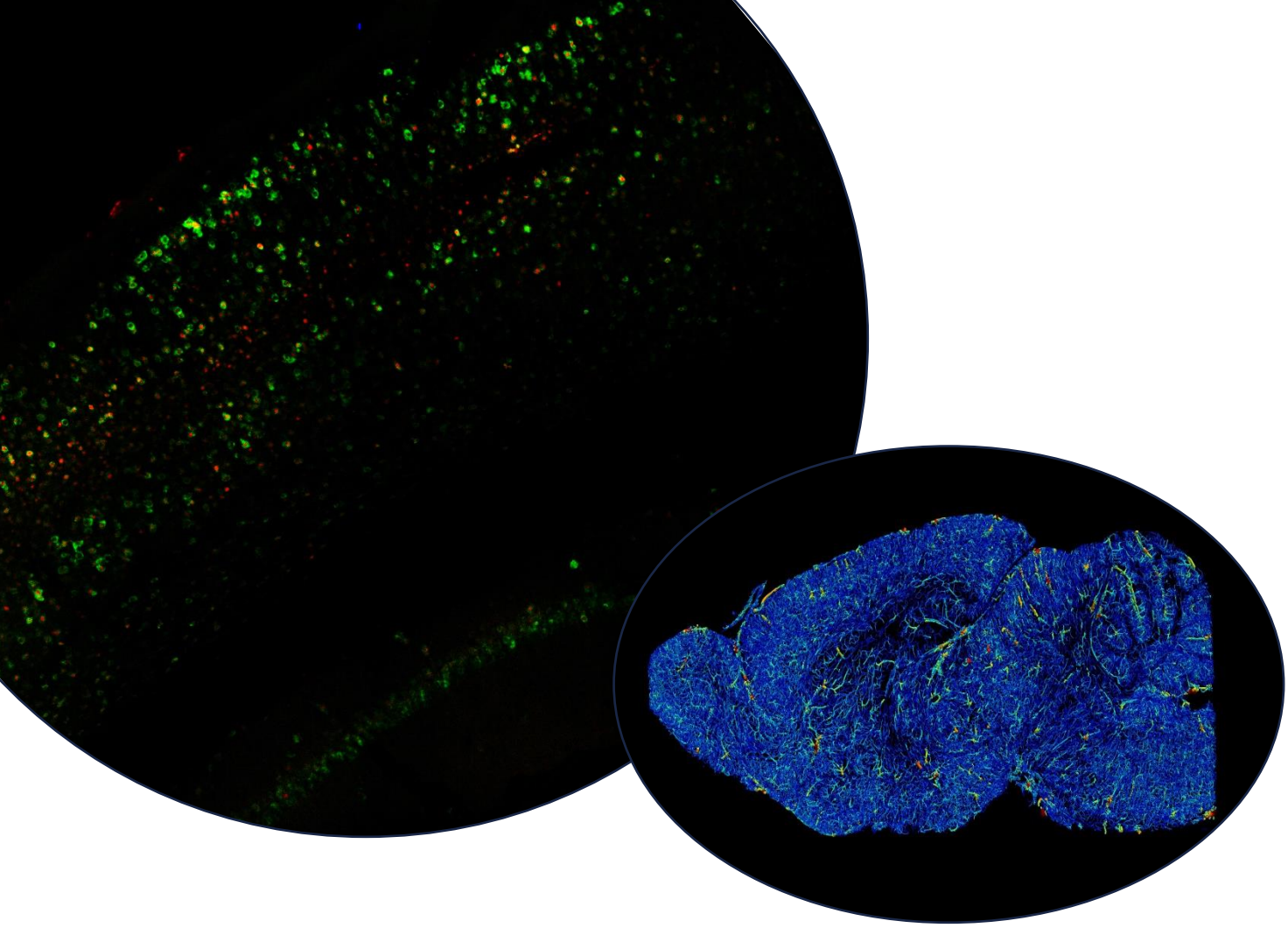

Sleep and cognition in rodents: Experience-dependent activity and spindle characteristics in the cortex

Author: D.C. Zantinge
Supervisor: Prof. Dr. Robbert Havekes
Daily supervisor: Dr. Julie Seibt
Date of completion: 29-08-2023

Sleep and cognition in rodents: Experience-dependent activity and spindle characteristics in the cortex

Title: Sleep and cognition in rodents: Experience-dependent activity and spindle characteristics in the cortex.
Author: D.C. Zantinge
Student number: S4744411, d.c.zantinge@student.rug.nl
Study: MSc. Biomedical Sciences - Neuroscience
Department: Faculty of Health and Medical Sciences, University of Surrey
Supervisors: Dr. Julie Seibt, Prof. Dr. Robbert Havekes
Date of completion: 29-08-2023

1. Abstract

Background: Sleep is a behavioural state essential for numerous brain functions, which consists of two main states, rapid eye movement (REM) and non-REM (NREM) sleep. Among the sleep oscillations important for cognition, NREM spindles (9-16Hz) have shown a strong correlation between variations in spindles and markers of cognitive functioning. However, how cognitive stimulation, such as exposure to an enriched environment, alters spindle events remains unknown. The relationship between cognitive processing and sleep has been studied thoroughly in rodents using the novel object recognition task (NORT). This task is primarily used to assess spatial memory in the hippocampus, but variants can be used to assess the relationship between sleep and cognitive processes in the cortex, which is much less studied. The first aim of this project is to establish a novel object recognition task focused on sensory stimulation in mice and determine the influence of sleep deprivation after learning on molecular markers of experience-dependent activity in the somatosensory cortex. The second aim is to characterise changes in spindle events across the 24-hour circadian time and in response to cognitive stimulation using enriched environment exposure.

Methods: For the first aim, mice were subjected to a NORT, for which half of the animals received 5 hours of sleep deprivation or not after testing. For measures of experience-dependent activity, animals were sacrificed immediately after acquisition, after 5 hours of sleep deprivation or after the testing session. Brains were then sectioned and immunohistochemically stained against c-Fos and PS6. For the second aim conducted in rats, to assess spindle activity, EEG of 8 animals were analysed. Spindle parameters were measured during a 24h baseline period and after a 3h exposure to an enriched environment.

Results: The results show a trend toward memory impairment due to sleep deprivation after learning, although these results did not reach significance. However, a significant increase in c-Fos and PS6 positively stained cells after learning and sleep deprivation was shown. Our spindle analysis did not show any significant differences for spindle amplitude, density, duration, or frequency after enriched environment exposure. Finally, no distinct circadian pattern was found in spindle amplitude, duration, and frequency, whereas density displayed a circadian rhythmicity of increasing during the first 9 hours of the dark phase and the last 8 hours of the light phase.

Conclusions: Our study shows that sleep deprivation induces an increase in cellular activity in the somatosensory cortex following a sensory perceptual learning test. However, sleep deprivation does not appear to influence object recognition. Our results also indicate that complex sensorimotor experience does not influence sleep markers of cognition, spindles specifically. However, our results indicate that some spindle characteristics, such as density follow a circadian rhythmicity. Future results could yield interesting results on investigating co-localization of c-Fos and PS6 in neurons specifically. Additionally, circadian spindle activity could be investigated during independent sleep stages instead of an overall 24-hour period.

Key words: Sleep, spindles, somatosensory cortex, NORT, EE, c-Fos, PS6

2. List of abbreviations

4EBP-1	= Eukaryotic translation initiation factor 4E binding protein 1
Akt	= protein kinase B
ANOVA	= Analysis of variance
ASRU	= Animals in Science Regulation Unit
AWERB	= Animal Welfare and Ethical Review Body
BRF	= Biomedical Research Facility
EE	= Enriched environment
EEG	= Electroencephalogram
ERK	= Extracellular signal-regulated kinases
FFT	= Fast Fourier Transformation
IEG	= Immediate Early Gene
i.p.	= Intraperitoneal
IS	= Intermediate stage
MAPK	= Microtubule associated protein kinases
mTOR	= Mammalian target of rapamycin
NGS	= Normal goat serum
NORT	= Novel object recognition task
NREM	= Non-REM
PBS	= Phosphate Buffered Saline
PFA	= Paraformaldehyde
PI3K	= Phosphoinositide 3-kinase
PS6	= Ribosomal protein S6
REM	= Rapid eye movement
S6K	= Ribosomal protein S6 kinases
SD	= Sleep deprivation
SEM	= Standard error of the mean
Ser	= Serine
ST	= Smooth texture

Table of contents

3. Introduction

Sleep is a behavioural state characterized by a reduced consciousness and responsiveness to external stimuli, which is essential for numerous brain functions such as memory formation, brain plasticity and thermoregulation (Anafi et al., 2019). Although many functions of sleep remain unknown, many species in the animal kingdom have shown to manifest sleep or a similar brain state (Le Bon, 2020). Sleep in mammals and birds consists of two main states, rapid eye movement (REM) sleep and non-REM (NREM) sleep. Sleep cycles constitute the alternation of both stages, where NREM transitions into REM sleep (Colavito et al., 2013; Rayan et al., 2022). Sleep is regulated in a 24-hour rhythm mediated by the circadian pacemaker, entrained to the light-dark cycle. This system ensures the ability to adapt to our environment and function properly (Reddy et al., 2023). Loss of sleep contributes to detrimental effects in bodily functions, such as an increased risk of disease, as well as brain functions, including a decrease of cognitive functioning. Studies have shown these detrimental effects through deprivation of either one or both sleep stages (Anafi et al., 2019; Cai et al., 2022).

When assessing sleep in rodents, the two sleep stages NREM and REM are characterized by changes in electrical signals that indicate brain activity, measured through an electroencephalogram (EEG). During REM sleep, the EEG indicates an increase in hippocampal theta activity (4-9 Hz), whereas an abundance of delta activity (0-4 Hz) and sigma (i.e., spindles) (9-15Hz) is shown during NREM sleep (Yamazaki et al., 2020). The transition from NREM sleep into REM sleep involves an intermediate state associated with an increase in hippocampal theta activity and spindles (Carrera-Cañas et al., 2019; Peyrache & Seibt, 2020). Spindles are a result of interplay between the thalamus and neocortex, and they are suggested to act as a mediator for general cognition and brain plasticity. The previously mentioned circadian rhythmicity of sleep has also been indicated to regulate spindle activity in humans, although this is not systematically researched in rodents. As sleep in rodents and humans is similar, it is suggested that a circadian rhythmicity for spindles is also present in rodents. Furthermore, studies have shown a strong correlation between cognitive tasks and variation in spindle characteristics such as density and frequency (Fernandez & Lüthi, 2020). As a result, it is suggested that cognitive stimulation could possibly alter characteristics and circadian rhythmicity of spindle events in turn.

This relationship between sleep and cognition has been studied in rodents by using various tasks. One such tasks is the novel object recognition task (NORT). The NORT is a well-established paradigm to assess working memory and memory consolidation in rodents (Antunes & Biala, 2012). This paradigm is mainly used to test spatial memory by changing the location of an object (Tudor et al., 2016), although it can be used to test other cognitive processes using perceptual novelty for example. In this task, an animal investigates a pair of identical objects initially during an acquisition period, after which one object is replaced by a novel object during a recognition phase. Due to a preference of rodents for novelty (Leger et al., 2013), the investigation of the novel object can be used to assess object recognition. Subsequently, the recognition memory can be assessed, similar to episodic memory in humans (Cordeira et al., 2018). Sleep loss after the acquisition phase induces deficits in recognition of objects by interfering with memory consolidation, especially during the first hours after acquisition (Tudor et al., 2016). Although previous studies mainly focused on the hippocampus through object-location memory, an alteration of the NORT can be used to focus on other brain areas such as the somatosensory cortex using somatosensory cues. Sensory experiences associated with novel object recognition are processed by the somatosensory cortex, such as the identification of shapes, sizes, and textures of objects (Raju & Tadi., 2022). Additionally, previous studies have shown a relationship between sleep and consolidation of perceptual learning (Miyamoto et al., 2016). Although the

effects of sleep deprivation on memory formation have been established, how sleep deprivation affects perceptual memory, involving the somatosensory cortex is poorly investigated.

Molecular markers can be used to study activation of specific cells in response to learning. Due to the complex mechanisms involved in learning, there is a wide variety of molecular markers available. Two examples of markers known to be induced by learning in cells are c-Fos and ribosomal protein S6 (PS6). Cellular activation leads to changes in expression of immediate early genes (IEGs) such as c-Fos, which is widely used as a marker of activity-dependent neuronal activity (Gallo et al., 2018). PS6 in turn is phosphorylated by ribosomal protein S6 kinase (S6K) after cellular activation. After phosphorylation, PS6 regulates modifications of proteins and induces protein synthesis (Graber et al., 2013), a mechanism essential for memory formation (Xia & Storm, 2017). The pathways involved in c-Fos and PS6 induction are depicted in figure 1. Studies have shown that learning increases phosphorylation of S6 in the hippocampus, whereas sleep loss induces a decrease (Delorme et al., 2021).

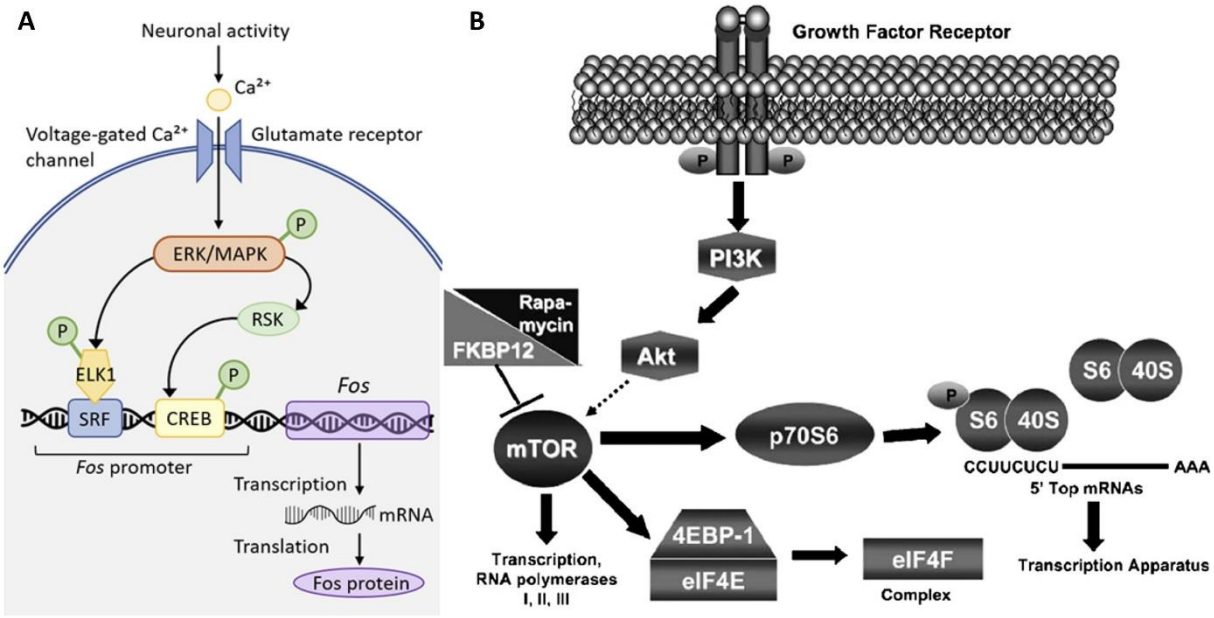

Figure 1: Pathways for induction of c-Fos and phosphorylation of PS6.
Neuronal activity as a result of learning induces translation of c-Fos (A). Neuronal activation leads to an influx of calcium through the glutamate receptor, which induces transcription of the Fos gene through extracellular signal-regulated kinases (ERK)/microtubule associated protein kinases (MAPK) activation. In terms of PS6 (B), learning induces activation of the growth factor receptor, which leads to activation of the phosphoinositide 3-kinase (PI3K)/protein kinase B (Akt) pathway. This pathway activates the target of the mechanistic target of rapamycin (mTOR), which in turn induces transcription of eukaryotic translation initiation factor 4E binding protein 1 (4EBP-1) and phosphorylation of S6 (Adapted from Iwenofu et al., 2008 and Adam Hall, 2020).

Hypothesis and aims:
The interaction between sleep and learning has been extensively studied in the rodent hippocampus, (Havekes & Abel, 2017). We hypothesise that similar changes, such as activity-dependent expression of markers of activity, occur in the cortex as well. By using a version of the NORT involving sensory perceptual learning and thus the cortex, we will test whether sleep deprivation following learning affects markers of activity (e.g., c-Fos and PS6) in the somatosensory cortex of mice. We also hypothesize that complex sensorimotor learning influences sleep markers of cognition, such as sleep spindles.

To address these hypotheses, the following aims were formulated:

1. Investigating the role of sleep in a sensory-dependent learning task. After validating the NORT focused on sensory stimulation in mice, we will determine the influence of sleep deprivation (SD) on activity in the somatosensory cortex.
    a. This will be investigated by sleep depriving animals after the acquisition phase in the NORT and assessing levels of PS6 and c-Fos activity after sleep deprivation compared to immediately after acquisition.
2. Determine the influence of cognitive stimulation and circadian rhythms on spindle events in rats.
    a. To investigate the influence of circadian time, 24h baseline EEG recordings will be scored and analysed.
    b. The influence of cognitive stimulation will be assessed using short term (3 hours) exposure to an enriched environment. Spindle characteristics will be compared between baseline and after cognitive stimulation.

4. Methods

4.1 Animals

For the NORT, 6 male heterozygous Rbp4-Cre and 10 wildtype Rbp4-Cre mice (2.5-6 months) were bred and group housed in green line Sealsafe® Plus cages (GM500). Object selection for the NORT was executed using 14 mice, which were a mixture of Rpl22, Rbp4-Cre and Rbp4-CreXRpl22 mice to reduce animal waste. Mice were not used for other experiments. In the EEG recording experiment 3 male and 5 female Lister Hooded rats were used (6-14 weeks). All animals had access to water and food *ad libitum* and were maintained under a 12:12-h light-dark cycle (lights on at 8:15 AM). All animals were handled daily from birth or arrival to the facility to minimize stressful responses during experiments. Experiments were executed during the light period. Furthermore, an ambient temperature of 21 ± 1°C was maintained with a humidity of 50 ± 5%. All procedures were conducted in accordance with guidelines approved by the Animals in Science Regulation Unit (ASRU) of the Home Office, the Animal Welfare and Ethical Review Body (AWERB) as well as the Biomedical Research Facility (BRF) at the University of Surrey.

4.2 Genotyping

To determine the genetic variant of each animal, a genotyping assay was executed. Tissue samples were bifurcated, one half was stored at -20 °C and the second half transferred to a PCR reaction tube. Tools were cleaned using 90% ethanol between tissue samples. Genotyping was performed using the Phire Tissue Direct PCR Master Mix (Thermo Fisher, F170S) according to the instruction. Each PCR reaction contained 1X Master Mix, 1 µL of isolated DNA, 10 µM of each Rbp4 primer and Millipore water to a final volume of 20 µL. Primers were synthesized by Merck (For: 5'-GGGCGGCCTCGGTCCTC-3', Rev: 5'-CCCCAGAAATGCCAGATTACGTAT-3'). The reactions were carried out in a PCR machine (GeneAmp®, 270S4070517) using the instructed conditions. To indicate the size of DNA in the samples, a GeneRuler Express DNA ladder (Thermo Fisher Scientific, SM1553) was used. Images of the gels were acquired using Image Lab software (version 6.0) for Nucleic Acid gel w/SYBR Safe application and a Gel Doc™ EZ Imager (Bio-Rad, 735BR06308).

4.3 NORT

4.3.1 Objects and set-up

Novel object recognition was assessed in a white polyvinyl open field box with a plexiglass bottom (36 cm x 27 cm x 30 cm). The arena was located in a dimly lit recording system (Zantiks, LT unit, Appendix 1) (41 cm x 56 cm x 87 cm), which provided infrared light from the bottom of the system. An overhead infrared video monitoring system recorded each session. Sample objects from cast acrylic were laser-cut by Zantiks (3.4 cm x 3.4 cm x 8 cm) and were similar in shape but different in colour or texture, or shaped as chess pieces (Appendix 1). Objects were placed in towers (10 cm x 10 cm x 30 cm) containing two holes on every surface (1 cm x 5 cm) at a height of 3 cm from the floor of the arena to allow exploration of the objects (Appendix 1). Additionally, objects were fitted into the towers to prevent displacement by the animals. Between animals, the arena, the towers, and the objects were cleaned using 70% ethanol to eliminate olfactory cues.

4.3.2 Preference and discrimination

To ensure exploration time of objects was comparable between objects in a pairing, a preference test was performed. Animals were habituated inside the empty arena for 5, 10, and 15 minutes for 3 consecutive days prior to the testing day. The preference test was executed by placing a single mouse into the arena with two non-identical sample objects for a period of 10 minutes to allow exploration of the objects. Animals with a total exploration time below 20 seconds were excluded from the results.

To ensure animals were able to discriminate between the objects in a pairing, a discrimination test was performed. Animals were habituated as stated in the preference test. The discrimination test was executed by placing a single mouse into the arena with two identical sample objects for a period of 10 minutes to allow exploration of the objects. After a 1-hour delay animals were returned to the testing arena with one familiarized object and a novel object for a period of 10 minutes. Animals with a total exploration time below 20 seconds were excluded from the results.

4.3.3 Novel object recognition paradigm and sleep deprivation

To determine the cognitive performance of animals, a novel object recognition paradigm was executed. The test was divided into an acquisition and recognition phase. The animals were habituated as stated previously in the preference and discrimination test. In the acquisition phase, animals were placed in the arena with two identical sample objects for three consecutive periods of 10 minutes. Between the acquisition periods, animals were placed back in their home cage for 10 minutes. Mice were tested for novel object recognition after a 24h interval by placement into the arena for 10 minutes with a familiarized object and a novel object. Mice assigned to the control experiment were placed in the arena without objects and towers during both the acquisition and recognition phase to prevent learning. Animals assigned to sleep deprivation received 5 hours of sleep deprivation following the acquisition phase. Mice were kept awake by gently tapping the home cage or direct contact by hand.

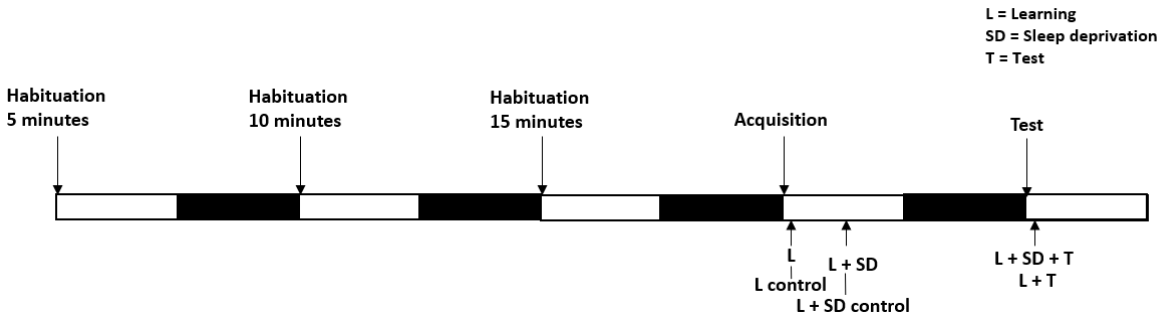

Figure 2: Experimental outline in novel object recognition.

Figure 2 depicts the experimental outline that was used in the NORT task with points of sacrifice for every group. Every animal underwent three consecutive days of habituation of 5, 10 and 15 minutes. On the fourth day, all animals underwent acquisition with or without objects (control). After acquisition two groups were sacrificed and two groups underwent SD and were sacrificed subsequently. The final two groups were subjected to a testing session on the fifth day and were sacrificed subsequently. Groups sacrificed on the fourth day were used for immunohistochemistry, groups sacrificed on the fifth day were used solely for novel object recognition.

4.3.4 Behavioural analysis

The time spent exploring each object was measured by recording time spent inside the object towers with the nose until complete removal from the towers. Time spent inside towers or sitting on the object were not defined as object investigation. Object preference during the preference test was determined by calculating the preference index as follows:

Preference/recognition index = Time spent at one object / Total exploration time for both objects.

Preference for an object was indicated by an animal spending significantly more time at one object in a combination. Object recognition during the discrimination test was calculated according to the above-mentioned calculation. Object recognition was indicated by an animal spending significantly more time at the novel object compared to the familiar object. The discrimination index for novel object recognition during the test was calculated as follows:

Discrimination index = (Time spent at novel object – Time spent at familiar object) / Total exploration time for both objects.

A higher discrimination index indicated the increased capability to distinguish between two objects in a combination.

Exploration times during novel object recognition were measured automatically using the Zantiks server, that recorded object exploration inside the towers, as well as manually. Results for exploration are based on the manual scoring due to inaccuracy of the Zantiks server. To analyse exploration times in novel object recognition, the discrimination and preference indices were calculated as mentioned previously. Statistical analysis was performed using GraphPad Prism 8.4.3 software (GraphPad Software, La Jolla California USA). To investigate the effect of sleep deprivation on novel object exploration, an independent-sample t-test with Welch's correction was performed. To further investigate the total exploration times between the acquisition and testing trials, a Welch analysis of variance (ANOVA) test was executed. Finally, to evaluate the agreement between the manual and automatic scoring by the system, a Pearson correlation was performed. Differences were considered significant if $p < 0.05$. In the Pearson correlation, the correlation was considered significant if $p < 0.05$.

4.4 Tissue collection

Tissue samples were collected after sleep deprivation or directly after the acquisition phase for a total of 10 animals. Mice were anaesthetized using isoflurane (Zoetis, IsoFlo®, 5%, O_2/NO_2) by placing the animal in a continuous anaesthetic induction chamber attached to an anaesthetic machine (Vet Tech, 942). After induction of anaesthesia, mice were moved to a surgical surface and the nose and mouth of the animals was placed inside an anaesthetic circuit. The anaesthesia was determined by assessing the response to toe pinches. When appropriate anaesthesia was determined, the thoracic cavity was opened using scissors, the ribcage was removed, and the heart was fully exposed. To remove blood from the system, the vena cava was incised and 30 mL of 1X Phosphate Buffered Saline (PBS) (Sigma, P4417) was first injected into the left ventricle at a constant speed using a 21-gauge needle (Terumo, NN-2138R) while turning off the anaesthetic machine. This was followed by the injection of 30 mL of 4% paraformaldehyde (PFA) (Thermo Scientific, J19943-K2). After perfusion, mice were decapitated, and the skull was opened. The brain was removed using a spatula and stored on ice in 4 mL of 4% PFA. After 5 hours, the brains were washed 2 times using 1X PBS and transferred to a 15% sucrose solution (Sigma-Aldrich, 16104) in 1X PBS and stored at 4 °C. Brains

were transferred a second time after 24-36 hours to a 30% sucrose solution in 1X PBS and stored at 4 °C. Subsequently brains were placed in an iron tissue mold (Leica, 0388 32453), and frozen in optimal cutting temperature compound (CellPath, KMA-0100-00A) and stored at -80 °C for further analysis.

4.5 Immunohistochemistry

To determine the influence of SD after the acquisition phase on cellular activity across the cortex, immunohistochemical analysis was executed. Using a cryostat (Leica, 7998), 50 µm frozen brain sections were obtained and collected free-floating in a 1X PBS solution. The object temperature was set to -18 °C while the chamber temperature was set to -15 °C. Tissues were subsequently washed 3 times with 1X PBS, 5 minutes each. After this, tissues were treated with permeabilization buffer containing a 1:1 dilution of 99.8% ethanol (Merck, 64-17-5) and 1X PBS. Subsequently, tissues were co-stained overnight at 4 °C with primary antibodies for Phospho-S6 (Serine (Ser) 244/247) (Thermo Fisher Scientific, 44-923G, 1:1500) and c-Fos (Abcam, ab208942, 1:2000) diluted in 1X PBS with 1% normal goat serum (NGS) (Vector laboratories, S-1000-20) and 0.1% Triton X-100 (Sigma, T8532). Tissues were then washed 4 times with 1X PBS, 5 minutes each, and incubated with a 1:2000 secondary antibody dilution for Alexa Fluor 488 (Invitrogen, A21206) and Alexa Fluor 555 (Invitrogen, A32727) diluted in 0.1% Triton X-100/1% NGS for 90 minutes at 4 °C. Subsequently, tissues were washed 4 times with 1X PBS, 5 minutes each, and mounted using Vectashield (Vector Laboratories, H-2000) and cover slipped.

Antibody concentrations for Phospho-S6 (Ser 234/235), Phospho-S6 (Ser 244/247) and c-Fos were determined using the above-mentioned protocol. Experimental brain sections were probed with the primary antibodies for Phospho-S6 (Ser 235/237) (Cell signaling, 4858, dilutions 1:50 and 1:200), Phospho-S6 (Ser 244/247) (Dilutions 1:750 and 1:1500) and c-Fos (Dilutions 1:500, 1:1000 and 1:2000). Obtained images are depicted in Appendix 2.

4.6 Image acquisition and analysis

Images were captured using an inverted confocal microscope (Nikon, 636683). Settings for light and the camera were controlled using Nikon Elements Confocal software (Elements Package). Images were taken at a 20X objective lens using lasers at 405 nm, 488 nm, and 561 nm for blue, green, and red channels. Images obtained from immunohistochemistry were processed in ImageJ software (v1.54d) by separating the image by colour channel. Cells were then visually identified and counted for three areas of 500 by 500 µm and expressed as counts/mm^2. Statistical analysis was then performed using GraphPad Prism by performing a non-matched Welch ANOVA test for the comparison of staining after SD and immediately after learning. Differences were considered significant if $p < 0.05$.

4.7 EEG acquisition in enriched environment (EE) exposure in rats

The following procedures were executed in 2017 before the beginning of the relevant project of this report and carried out by Lucas Santos. Data analysation and further statistics were executed by the experimenter.

4.7.1 EEG telemetry surgery

Surgery on rats was performed under general anaesthesia (5% isoflurane, O_2/NO_2) and aseptic conditions. After induction of anaesthesia, animals were kept under inhalation anaesthesia (2-2.5% isoflurane in 1:2 O_2:N_2O overflow). The skin of the scalp was shaved, and animals received an injection of buprenorphine (Hikma, 0143-924-05, 0.01-0.05 mg/kg, intraperitoneal (i.p.)) in combination with meloxicam (Metacam, 113027, 0.01-0.05 mg/kg, i.p.). Subsequently, the animal was moved to a sterile surgical surface under

anaesthesia and moisturizer was applied to the eyes (EMLA, 100048). The skin was cleaned using chlorhexidine (Hibiscrub, LCKW8) and an incision was made along the midline of the scalp to expose the skull. The skull was cleaned using 3% H_2O_2 (McKlords industrial) and four 0.5 mm holes were drilled, two at the frontal lobe at 2 mm from the midline on either side, one at the parietal lobe at 2 mm from the midline and one at the occipital lobe 4 mm posterior of the parietal hole. EEG screws were inserted into the holes and the end of the EEG wires was twisted around the screws. The screws were then covered with dental cement (3M™, 123-0005) and the wires were covered with Kwik-Cast (WPI, 08C). An incision was made caudal to the scalp incision and the EEG transmitter (DSI™, HD-X02) was placed subcutaneously with any excess wires. Subsequently the caudal incision as well as the scalp incision was sutured using non-absorbable 6-0 Vicryl sutures.

After surgery animals received meloxicam (0.01-0.05 mg/kg, orally) for 3 consecutive days as animals were monitored for weight and welfare.

4.7.2 EE exposure and EEG recordings

Experiments were commenced after at least one week of recovery. The implant was used to record EEG traces at a sampling rate of 500 Hz at the start of the dark phase. Following a 24-hour baseline recording in the home cage, animals were exposed to an EE cage (ViewPoint, Marlau cage™) for three hours at the end of the following dark phase (ZT 21-ZT24). After EE exposure, animals were returned to their home cage and left to sleep *ad libitum* for three more hours before they were sacrificed using the method of perfusion mentioned in 4.4 for additional molecular analysis (not used in this project). During the experiment, activity of the animals was tracked using a DSI signal interface (MX2, 1154084) with Ponemah software (DSI, v5).

4.7.3 Data analysis and statistics

Sleep traces obtained from rats were used to investigate spindle density, frequency, amplitude, and duration. EEG traces were filtered (high-pass filter: 0.50 Hz, low-pass filter: 30 Hz) and subjected to a Fast Fourier Transformation (FFT). EEG traces were then visually scored in 4-second epochs aided by EEG power values and activity parameters. Epochs were scored as Wake, NREM, REM and intermediate stage (IS) using SleepSign (Kissi Comtec, v3.3.7) as previously performed by Seibt et al. (2017). Subsequently, traces were analysed using MATLAB R2023a (MathWorks, v9.14) to investigate spindle amplitude, density, duration, and frequency across sleep stages during the 24-hour baseline period and the 3-hour period post EE. Furthermore, spindle amplitude, density, duration, and frequency were determined over the 24-hour baseline period in 1-hour bins. Individual spindles were detected using the sleepwalker Toolbox (https://gitlab.com/ubartsch/sleepwalker). A one-way ANOVA was performed to investigate changes in spindle characteristics between the baseline and post EE using GraphPad.

5. Results

5.1 Object selection prior to the NORT

To establish the object selection to be used in the NORT we performed a preference and discrimination test. Mice were placed in an arena with two different objects (preference test) or two identical objects (discrimination test) for 10 minutes. In the discrimination test animals were placed in the arena for an additional 10 minutes after a 60-minute interval with a familiar and a novel object. Subsequently we calculated the preference and recognition index for each possible object combination based on exploration times as mentioned in 4.3.4. Each object combination with their corresponding index is depicted in Fig. 3.

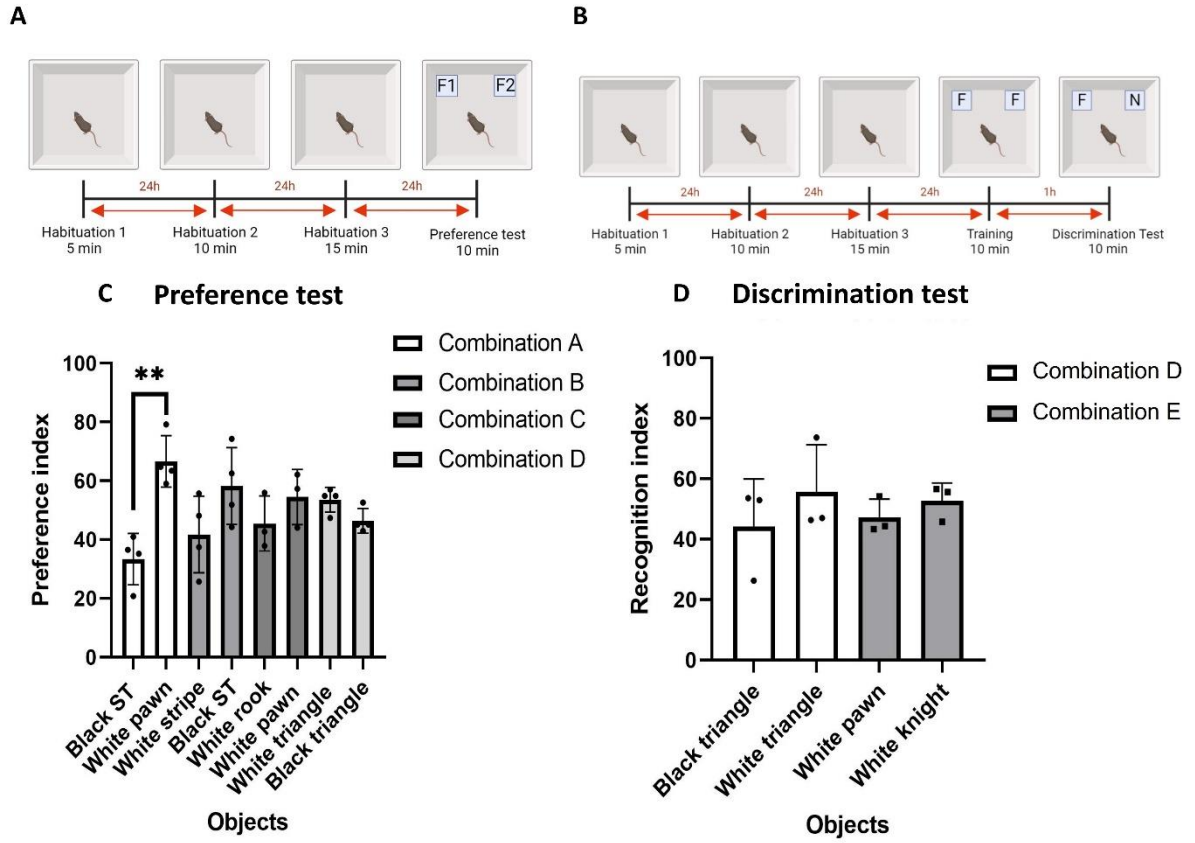

Figure 3: Pilot studies per object and combination for object selection.

Experimental set-up for the preference (A) and the discrimination (B) test consisting of habituation, training, and testing phase, including time interval and time accounted for each session. Preference indices and recognition indices are shown for object combinations A (white), B (grey), C (dark grey), D (light grey in figure C, white in figure D), and E (grey, figure D) for the preference test (C) and the discrimination test (D). The indices are plotted against the objects. Data are shown as mean ± standard error of the mean (SEM) (n = 4 (C), n = 3 (D)). Stars indicate significant differences between two objects in a combination (P < 0.005 (**), Welch ANOVA). Significant differences were found in the preference index between the black object with a smooth texture (ST) and the white chess pawn.

In the preference test (Fig. 3C) one combination of objects appears to induce a preference, which is combination A. The objects used in combination A are a black smooth textured object and a white chess pawn (see Appendix 1). In this object combination, the preference index for the black object is 32, whereas this is 65 for the white pawn, indicating a preference for the white pawn. Combinations B, C, and D did not induce a preference for one object and were suitable in the NORT. Additionally, observed from the

discrimination test (Fig. 3D) is that animals were not able to differentiate between object combinations D and E based on the recognition index. Results indicate a higher discrimination ability between the black and white triangled object (see Appendix 1) compared to the white chess pawn and white chess knight. Based on the results of the preference and discrimination indices, the combination of black and white triangled object was chosen for further execution of the NORT.

5.2 Object exploration during the NORT

The next step in our analysis was to investigate exploration time of objects in the NORT during the acquisition and test phases. Mice were placed in the arena with two identical objects for three consecutive training trials of 10 minutes as acquisition. Half of the animals were subjected to 5 hours of sleep deprivation after acquisition to test the requirement for sleep after learning for memory consolidation. After 24 hours, memory was tested by placing the animals in the arena with one familiar and one novel object. The exploration times for each object were determined using the Zantiks server as well as manual scoring from videos. Subsequently, the exploration times were used to calculate the discrimination index. The exploration times measured during each training and testing session and the recognition of novel objects are depicted in Fig 4. Additionally, the correlation between the manual and automated scoring was determined to investigate the accuracy of scoring by the system, which is depicted in Fig 4.

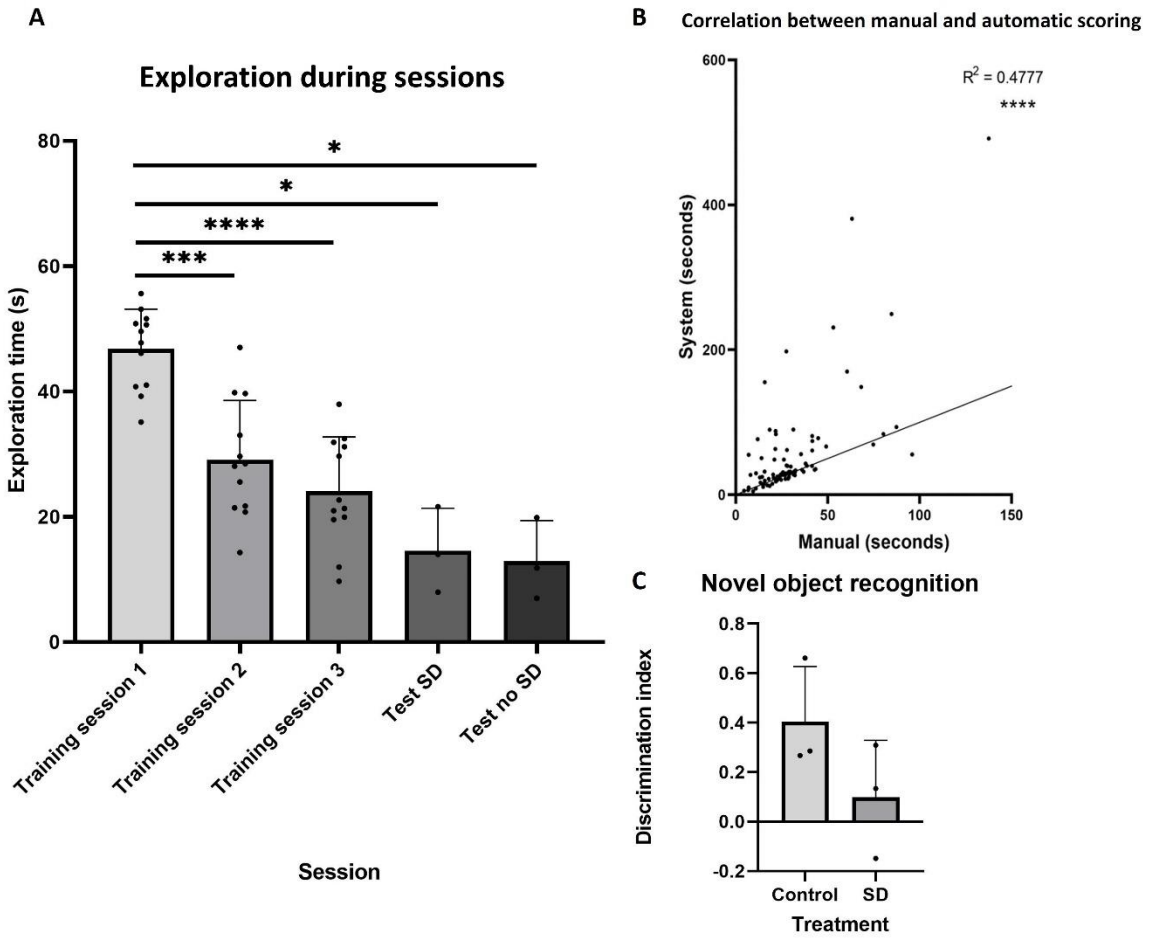

Figure 4: Exploration times and discrimination of the NORT.

The total exploration times during each session (A), the correlation between manual exploration scoring and scoring by the system (B) and the discrimination index for SD animals and non-SD animals (C). The exploration times are plotted against the sessions (A), automatically scored exploration times against manual scoring (B) and the discrimination indices against the treatment (C). Data are shown as mean + SEM or individual datapoints (n = 10 for training sessions and n = 3 for testing sessions (A), n = 10 (B), n = 3 (C)). Stars indicate significant differences between exploration times (P < 0.05 (*), P < 0.0005 (***), P < 0.00005 (****), Welch ANOVA (A) or a significant correlation (P < 0.00005 (****)), Pearson correlation (B). The R^2 for the Pearson correlation is shown in the top of the graph (B). Significant differences were found between exploration times for the first training session and every other training and testing session. Furthermore, a significant correlation between manual and automatic scoring was found.

Total exploration times of the objects by the animals (Fig. 4A) follows a significantly declining trend when comparing the first training session to other sessions. During the first training session, animals explored 45 seconds on average, which decreases to approximately 30 seconds during the second training session. Interestingly, exploration times do not decrease further after the second training session. Additionally, animals that received SD or no SD both explored the same amount of time (15 seconds) during the testing session, suggesting no influence of SD on exploration time.

As mentioned previously, the exploration times were determined both manually and using automatic scoring. The Pearson correlation (Fig. 4B) indicates a highly significant correlation and a medium positive correlation between the two methods ($R^2 = 0.4777$). The figure indicates a frequent overestimation of the exploration times by the Zantiks server compared to manual scoring.

Finally, discrimination indices of sleeping and SD animals (Fig. 4C) appears to indicate a slight difference in object recognition. Animals subjected to SD depict a discrimination index of 0.08, whereas animals that could sleep after learning depict a discrimination index of 0.4. However, this difference is not significant. This suggests that SD does not appear to influence recognition of objects in the NORT.

5.3 Cortical c-Fos and Phospho-S6 cell count

We then assessed changes in experience-dependent activity markers in the somatosensory cortices right after learning and learning followed by SD. Learning was performed as previously described and animals were sacrificed immediately after the training trials (No SD) or were subjected to 5 hours of sleep deprivation after training and then sacrificed (SD). Control groups underwent identical training sessions without objects and received identical treatments. An immunohistochemical protocol was executed on brain sections using primary antibodies for c-Fos and PS6. Positively stained cells were then counted manually. In Fig. 5 the cell density for c-Fos and PS6 positive cells is depicted for all groups.

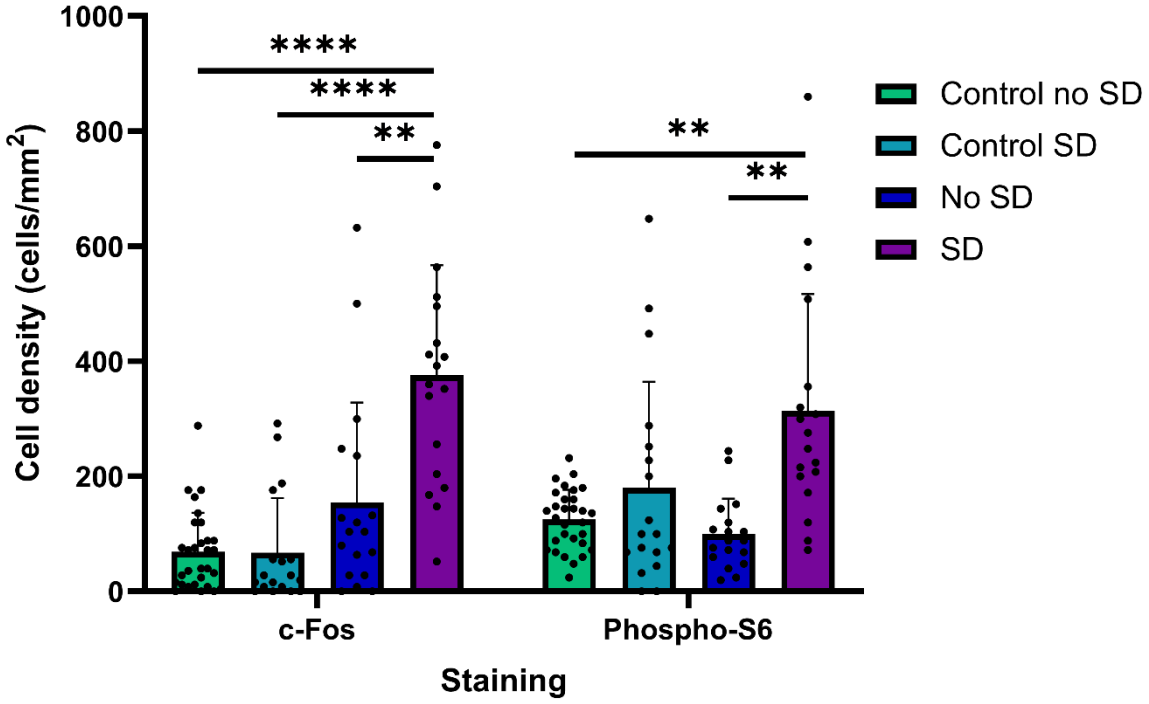

Figure 5: Cell counts for c-Fos and Phospho-S6 staining in the somatosensory cortex.
Changes in positively stained cells for c-Fos (left) and Phospho-S6 (right). Changes are shown for control groups without (green) and with (light blue) SD. Additionally, changes are shown for learning animals that did not receive SD (blue) and animals that did (purple). Data are shown as mean + SEM (n = 2 for controls, n = 3 for SD and no SD). Stars indicate significant differences in cell count between groups (P < 0.005 (**), P < 0.00005 (****), Welch ANOVA). Significant differences were found between SD animals and non-SD animals for both stainings as well as between SD animals and the control animals that did not receive SD. Additionally, changes in c-Fos activity were found between experimental animals that were subjected to SD and the control group that received SD.

The number of cells stained positively for c-Fos and PS6 increase in animals that underwent 5 hours of SD after learning compared to animals sacrificed right after learning from 100-150 cells/mm^2 to 300-390 cells/mm^2. For both markers this is also increased in SD animals compared to animals that did not receive learning and did not receive SD. The number of positively stained cells for c-Fos increased by approximately 330 cells/mm^2, whereas the number of cells positively stained for PS6 increased by approximately 200 cells/mm^2. The number of cells that were labelled positively for c-Fos in animals subjected to SD is also increased compared to control animals that did receive SD, whereas in PS6 this difference is not evident. These results indicate that SD induces an increase in c-Fos and PS6 after a learning event. Interestingly, activity of PS6 also appears to be elevated after SD in control animals.

5.4 Experience-dependent changes in spindle characteristics

Our following analyses focused on the results acquired from EEG recording in rats. To investigate the changes in spindle characteristics as a result of cognitive stimulation, animals were exposed to EE conditions while measuring EEG activity in the parietal and frontal EEGs. Recordings were then scored for sleep (NREM, REM, IS) and wake states. Detected spindle events were investigated over the 24h baseline period as well as 3h post EE exposure. The results of the analysis are depicted in Fig. 6.

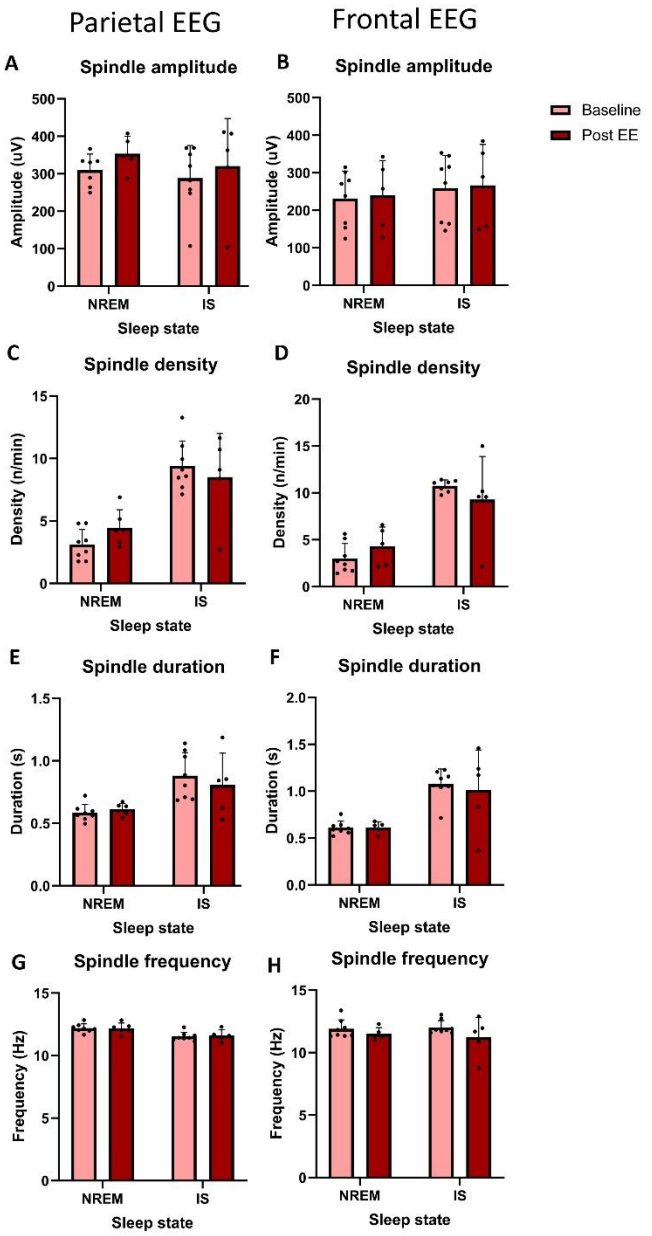

Figure 6: Spindle characteristics during baseline and post EE.

Changes in spindle characteristics during baseline (light pink) and during 3h post EE (dark pink). Characteristics shown are the amplitude (A, B), density (C, D), duration (E, F) and frequency (G, H) for the parietal (left panel) and frontal (right panel) EEG. Data are shown as mean ± SEM (n = 8 for baseline, n = 6 for post EE). No significant differences were found.

A non-significant increase in spindle amplitude appears to be shown in the parietal EEG (Fig 6A) post EE during each sleep stage. Interestingly, this difference is not shown in the frontal EEG (Fig 6B). Both results indicate a spindle amplitude in both sleep stages between 220 uV and 300 uV under baseline conditions and 220 uV and 350 uV post EE. Additionally, spindle amplitude in the frontal EEG appears to be decreased compared to the parietal EEG. Spindle density under baseline conditions (Fig 6C/D) appears to increase in IS compared to NREM under baseline conditions. This trend is also seen post EE in the parietal EEG, however not in the frontal EEG. Duration of spindles appears to increase during IS compared to NREM in both EEGs (Fig 6E/F). The duration spans between 0.55 seconds to 0.8 seconds in the parietal lobe, whereas this duration spans 0.6 seconds to 1.05 seconds in the frontal lobe. Finally, spindle frequency does not appear to follow a specific trend. In both EEGs (Fig 6G/H) spindle frequency spans from 10 Hz to 12.5 Hz and does not show variations, irrespective of sleep stage. Overall, spindle amplitude, density, duration, and frequency do not change significantly within 3h after cognitive stimulation.

5.5 Circadian-dependent changes in spindle characteristics

The final step in our analysis was the investigation of circadian rhythmicity of spindle characteristics across a 24h baseline period. The results of the analysis are depicted in Fig. 7.

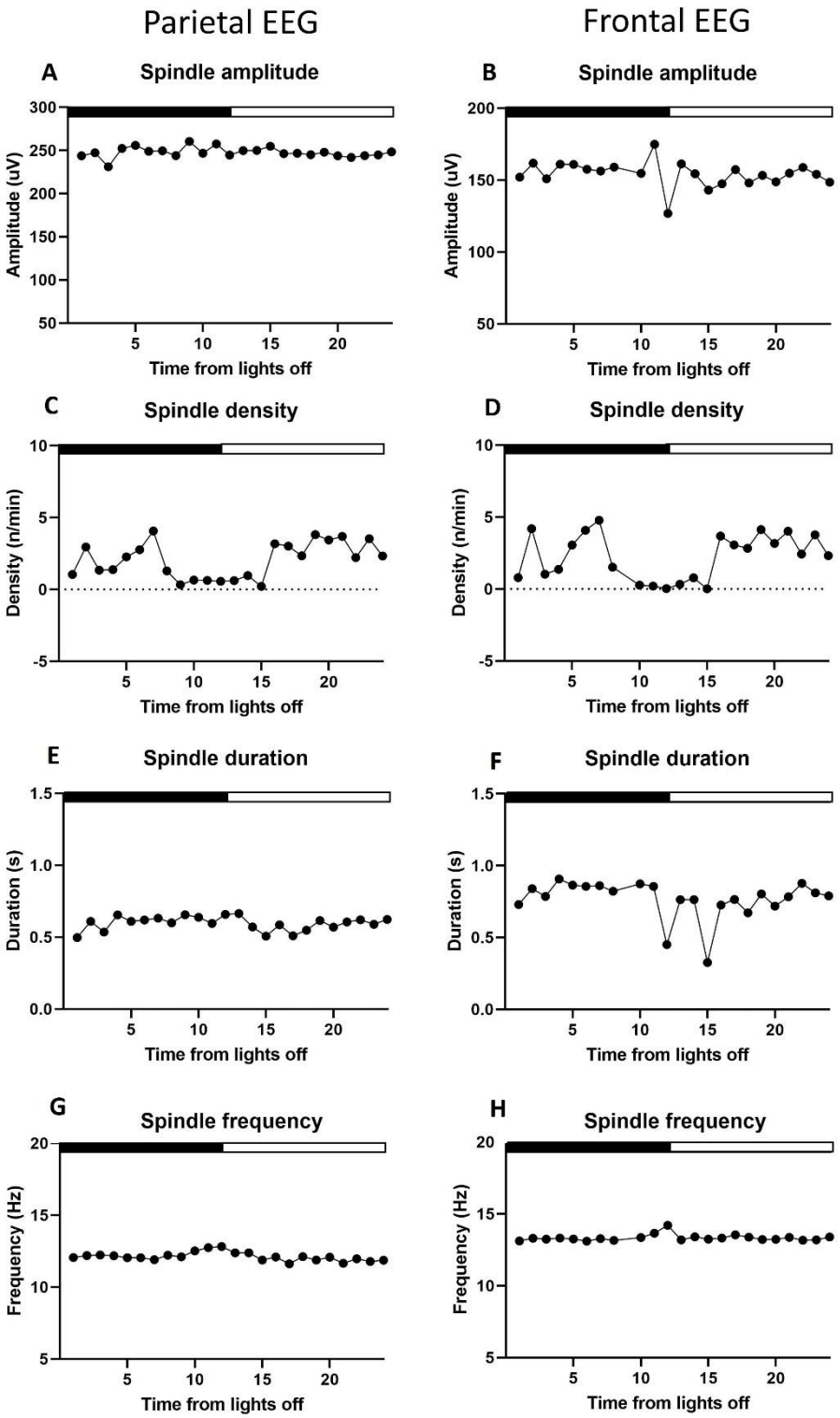

Figure 7: Circadian rhythmicity of spindle characteristics.

Circadian rhythmicity of spindle characteristics from the parietal lobe (left panel) and the frontal lobe (right panel) during a 24h baseline period. Characteristics shown are the amplitude (A, B), density (C, D), duration (E, F) and frequency (G, H). Data are shown as the mean (n = 8) due to time limitations in analysis.

In terms of circadian rhythmicity, it appears that spindle amplitude, duration, and frequency show no circadian pattern. Amplitude of the frontal EEG (Fig 7B) appears to be declined by 100 uV compared to the parietal EEG (Fig 7A), although this difference is not shown in other characteristics such as the duration (Fig 7E/F) and the frequency (Fig 7G/H). Duration averages between 0.5 to 0.9 seconds and the frequency averages between 12 and 14 Hz. The characteristic that shows a distinct circadian rhythmicity is the spindle density (Fig 7C/D). Spindle density appears elevated during the first 9 hours of the dark phase and again after 15 hours, during the last 8 hours of the light phase. A distinct decline is shown between these times to almost 0 n/min. A spindle density of 0 n/min also corresponds to a decrease in spindle duration and amplitude in the frontal EEG. Overall, spindle amplitude, duration and frequency do not show a distinct circadian pattern, whereas spindle density appears to decline during the final hours of the dark phase and the first hours of the light phase.

6. Discussion

The aim of this study was to assess the role of sleep in a sensory-dependent learning task. After validating the NORT focused on sensory stimulation in mice, we determined the influence of SD on activity in the somatosensory cortex. Our results indicate that SD appears to induce a slight reduction of object recognition, although this reduction is not significant. Furthermore, our results show that in our sensory perceptual version of the NORT, object exploration reduces after the first training session. In terms of activity-dependent markers in the somatosensory cortex, animals subjected to SD showed an increase of c-Fos and PS labelled cells compared to non-SD and non-learning animals. A second aim of this study was to determine the influence of cognitive stimulation and circadian time on spindle events in rats, using EE. Our results indicated that there were no significant changes in any spindle characteristics after 3h of cognitive stimulation during spindles rich sleep states (NREM and IS). Finally, no characteristics indicated a clear circadian rhythmicity except for spindle density over a baseline period of 24h.

As mentioned previously, SD appears to induce a slight reduction of object recognition, although this reduction was not significant. The discrimination index reached a mean value of 0.08 in animals that were subjected to 5 hours of SD after acquisition, whereas a mean value of 0.4 was reached in animals allowed to sleep after learning. Although it aligns with, it does not replicate earlier studies, which reported a clear impairment of object recognition due to SD (Jiao et al., 2022; Tudor et al., 2016). This is most likely due to our results being underpowered with 3 animals in each group, which is a particularly small sample size. According to a power analysis (G*Power 3.1.9.7), a sample size of at least 5 animals would be needed to reliably draw conclusions in our experiment. Although our results appear promising, it would be favourable in a future study to increase this number.

At the molecular level, our results indicate a baseline level of c-Fos activation of 50 cells/mm^2 and a baseline level of PS6 activation of 140 cells/mm^2 in the somatosensory cortex. In the SD condition, this increases to 180 cells/mm^2. The relatively high level of baseline PS6 is most likely due to the miscellaneous nature of PS6, for example in protein translation (Biever et al., 2015). Additionally, whereas learning appears to induce an increase in c-Fos activation, a slight decrease in PS6 stained cells is observed. This increase of c-Fos expression immediately after learning is in line with earlier studies that indicate an elevation in c-Fos positively stained cells in a stimulated area (Filipkowski et al., 2006). However, previous studies have shown an increase of PS6 in the hippocampus (Delorme et al., 2021) after learning, and especially after sleep following learning. Our results suggest that SD induces phosphorylation of PS6 in the somatosensory cortex, potentially during exploration of the home cage. Unfortunately, we did not add a group of animals allowed to sleep after learning, which is necessary to make confident conclusions based on our results. It would be interesting in a future study to investigate the activation of c-Fos and PS6 after a period of freely sleeping following learning. Finally, our results indicate that 5 hours of SD after learning induces an increase in c-Fos and PS6 in the somatosensory cortex compared to directly after learning. This result corresponds with a study by Delorme et al. (2021), which showed an increase of PS6 positive neurons in the primary somatosensory cortex after 3 hours of SD. Our results suggest that SD induces and increase in phosphorylation of S6, possibly as a result of learning before the start of SD. Overall, our results suggest that learning prior to SD induces an increased activation of cells in the somatosensory cortex. However, this conclusion can not be confidently made without adding a group of animals allowed to sleep freely.

Although our results indicate an increase cellular activation in the somatosensory cortex, future studies could be directed specifically at co-localisation of c-Fos and PS6. C-Fos and PS6 are often expressed after a variety of stimuli in both neurons and glial cells. It would be interesting to investigate the number of neurons

activated through this learning process using a neuronal marker. Additionally, it would be interesting to investigate neuronal activations through different layers of the somatosensory cortex as well as the co-localisation of both activity-dependent markers.

The increase in c-Fos after learning in the somatosensory cortex suggests that the tested paradigm provides sensory perceptual learning. In conjunction with a discrimination ability of objects, this paradigm appears to successfully contribute to investigate the relationship between sleep and memory. However, other results suggest that the number of training sessions induces a disinterest for objects. Our results suggest that the number of training sessions induces a disinterest for objects. A future direction would be to decrease the number of training sessions to 2 consecutive sessions of 10 minutes. This provides the possibility for animals to familiarize with objects without losing interest. In addition, this potentially increases object exploration during the testing session with a possible impact on the object discrimination scores. Additionally, it has been shown that light conditions affect synaptic plasticity, resulting in varying efficacy of spatial memory in the light and dark phase (Schröder et al., 2023). Object exploration in this study was executed during the light phase. It is suggested that executing the NORT during the dark phase possibly induces a more effective object exploration and object discrimination due to a more successful working memory. It would be interesting to investigate this effect in a future study. During this project, object exploration was assessed both manually and automatically. The correlation of results obtained with both approaches indicated a frequent overestimation of the system, which resulted in a correlation of 0.4777. This is due to the system inaccurately scoring exploration times when animals were at the other side of the arena, scoring time spent on top of objects as exploration and scoring exploration as animals were only touching the towers on the outside. It can be concluded that, currently, the automated system is inaccurate in scoring object exploration and that manual assessment is necessary.

The second aim of this study was to determine the influence of cognitive stimulation and circadian time on sleep spindle events in rats. Studies have shown that sleep-dependent memory consolidation increases spindle density and frequency (Hahn et al., 2019), which our results do not support. Other studies have also shown an increase in spindle duration and amplitude during sleep after a learning event (Schabus et al., 2004). However, this is likewise not supported by our results. Our results indicated no significant influence of EE on any characterstics during NREM or IS. It would be interesting to investigate changes in spindle activity after a longer time span of exposure to EE. Additionally, sleep stages post EE are compared to sleep stages in a 24h baseline period. A future direction would be to investigate the differences between the 3h post EE as well as 3h of the same circadian timing during the baseline period. This could potentially provide a smaller window of time which may lead to a decreased variability in the baseline measurements.

Our final analysis derived from EEG recordings was focused on determining the circadian rhythmicity of spindle characteristics. Our results suggest that spindle amplitude, duration and frequency do not show a distinct circadian pattern, whereas spindle density shows a circadian pattern which appears to decline during the last 3 hours of the dark phase and the first 4 hours of the light phase. Early studies have implicated a partly circadian rhythmicity for sleep spindle activity, mostly through a change in frequency (Dijk, 1995). However, whereas our study focused on an overall 24h period, this study focused on spindle activity specifically during NREM. It would be interesting to investigate spindle activity and characteristics during each independent sleep stage as well. This rhythmicity might become more evident from focusing on specific sleep stages instead of a 24h period overall. Additionally by focusing on individual animals instead of an 8 animal mean, which was a result of time limitations during the analysis.

In conclusion, this study shows that sleep may be important for object recognition in our sensory perceptual learning variant of the NORT provided an increase in subject number. However, we show that sleep deprivation induces an increase in markers of activity-dependent cellular activity in the somatosensory cortex. These results support the hypothesis that sleep deprivation affects somatosensory processing provided that a group of freely sleeping animals after learning is added. Additionally, our results indicate that complex sensorimotor learning does not influence sleep markers of cognition, spindles specifically. Finally, our results do not support the findings that spindle frequency is mediated by a circadian pacemaker, however a circadian pattern of spindle density was found. Future research could yield interesting results on specifically investigating neuronal activation in the somatosensory cortex, spindle activity during independent sleep stages, and the possible circadian rhythmicity of characteristics of spindle events.

7. Bibliography

Anafi, R. C., Kayser, M. S., & Raizen, D. M. (2019). Exploring phylogeny to find the function of sleep. *Nature Reviews Neuroscience*, *20*(2), 109–116. https://doi.org/10.1038/s41583-018-0098-9

Antunes, M., & Biala, G. (2012). The novel object recognition memory: Neurobiology, test procedure, and its modifications. *Cognitive Processing*, *13*(2), 93–110. https://doi.org/10.1007/s10339-011-0430-z

Biever, A., Valjent, E., & Puighermanal, E. (2015). Ribosomal protein S6 phosphorylation in the nervous system: From regulation to function. *Frontiers in Molecular Neuroscience*, *8*(DEC). https://doi.org/10.3389/fnmol.2015.00075

Cai, G., Lu, Y., Chen, J., Yang, D., Yan, R., Ren, M., He, S., Wu, S., & Zhao, Y. (2022). Brain-wide mapping of c-Fos expression with fluorescence micro-optical sectioning tomography in a chronic sleep deprivation mouse model. *Neurobiology of Stress*, *20*. https://doi.org/10.1016/j.ynstr.2022.100478

Carrera-Cañas, C., Garzón, M., & De Andrés, I. (2019). The transition between slow-wave sleep and REM sleep constitutes an independent sleep stage organized by cholinergic mechanisms in the rostrodorsal pontine tegmentum. *Frontiers in Neuroscience*, *13*(JUL). https://doi.org/10.3389/fnins.2019.00748

Colavito, V., Fabene, P. F., Grassi-Zucconi, G., Pifferi, F., Lamberty, Y., Bentivoglio, M., & Bertini, G. (2013). Experimental sleep deprivation as a tool to test memory deficits in rodents. *Frontiers in Systems Neuroscience*, *7*(DEC). https://doi.org/10.3389/fnsys.2013.00106

Cordeira, J., Kolluru, S. S., Rosenblatt, H., Kry, J., Strecker, R. E., & McCarley, R. W. (2018). Learning and memory are impaired in the object recognition task during metestrus/diestrus and after sleep deprivation. *Behavioural Brain Research*, *339*, 124–129. https://doi.org/10.1016/j.bbr.2017.11.033

Delorme, J., Wang, L., Roig Kuhn, F., Kodoth, V., Ma, J., Martinez, J. D., Raven, F., Toth, B. A., Balendran, V., Vega Medina, A., Jiang, S., Aton, S. J., & Takahashi, S. (2021). Sleep loss drives acetylcholine-and somatostatin interneuron-mediated gating of hippocampal activity to inhibit memory consolidation. *Proceedings of the National Academy of Sciences*. https://doi.org/10.1073/pnas.2019318118/-/DCSupplemental

Dijk, D.-J. (1995). EEG slow waves and sleep spindles: windows on the sleeping brain. *Behavioural Brain Research*, *69*, 109–116.

Fernandez, L. M. J., & Lüthi, A. (2020). Sleep spindles: Mechanisms and functions. *Physiological Reviews*, *100*(2), 805–868. https://doi.org/10.1152/physrev.00042.2018

Filipkowski, R. K., Knapska, E., & Kaczmarek, L. (2006). c-Fos and Zif268 in Learning and Memory-Studies on Expression and Function. In *Immediate Early Genes in Sensory Processing, Cognitive Performance and Neurological Disorders* (pp. 137–158). Springer.

Gallo, F. T., Katche, C., Morici, J. F., Medina, J. H., & Weisstaub, N. V. (2018). Immediate early genes, memory, and psychiatric disorders: Focus on c-Fos, Egr1 and Arc. *Frontiers in Behavioral Neuroscience*, *12*. https://doi.org/10.3389/fnbeh.2018.00079

Graber, T. E., McCamphill, P. K., & Sossin, W. S. (2013). A recollection of mTOR signaling in learning and memory. *Learning and Memory*, *20*(10), 518–530. https://doi.org/10.1101/lm.027664.112

Hahn, M., Joechner, A. K., Roell, J., Schabus, M., Heib, D. P. J., Gruber, G., Peigneux, P., & Hoedlmoser, K. (2019). Developmental changes of sleep spindles and their impact on sleep-dependent memory

consolidation and general cognitive abilities: A longitudinal approach. *Developmental Science*, *22*(1). https://doi.org/10.1111/desc.12706

Hall A, c-FOS: Molecular biology & detection for analysis of neuronal activity. September 21, 2020. Consulted on August 14th, 2023 on: c-FOS: Molecular biology & detection for analysis of neuronal activity (lifecanvastech.com).

Havekes, R., & Abel, T. (2017). The tired hippocampus: the molecular impact of sleep deprivation on hippocampal function. *Current Opinion in Neurobiology*, *44*, 13–19. https://doi.org/10.1016/j.conb.2017.02.005

Iwenofu, O. H., Lackman, R. D., Staddon, A. P., Goodwin, D. G., Haupt, H. M., & Brooks, J. S. J. (2008). Phospho-S6 ribosomal protein: A potential new predictive sarcoma marker for targeted mTOR therapy. *Modern Pathology*, *21*(3), 231–237. https://doi.org/10.1038/modpathol.3800995

Jiao, Q., Dong, X., Guo, C., Wu, T., Chen, F., Zhang, K., Ma, Z., Sun, Y., Cao, H., Tian, C., Hu, Q., Liu, N., Wang, Y., Ji, L., Yang, S., Zhang, X., Li, J., & Shen, H. (2022). Effects of sleep deprivation of various durations on novelty-related object recognition memory and object location memory in mice. *Behavioural Brain Research*, *418*. https://doi.org/10.1016/j.bbr.2021.113621

Le Bon, O. (2020). Relationships between REM and NREM in the NREM-REM sleep cycle: a review on competing concepts. *Sleep Medicine*, *70*, 6–16. https://doi.org/10.1016/j.sleep.2020.02.004

Leger, M., Quiedeville, A., Bouet, V., Haelewyn, B., Boulouard, M., Schumann-Bard, P., & Freret, T. (2013). Object recognition test in mice. *Nature Protocols*, *8*(12), 2531–2537. https://doi.org/10.1038/nprot.2013.155

Miyamoto, D., Hirai, D., Fung, C. C. A., Inutsuka, A., Odagawa, M., Suzuki, T., Boehringer, R., Adaikkan, C., Matsubara, C., Matsuki, N., Fukai, T., Mchugh, T. J., Yamanaka, A., & Murayama, M. (2016). Top-down cortical input during NREM sleep consolidates perceptual memory. *Science*, *352*(6291). https://www.science.org

Peyrache, A., & Seibt, J. (2020). A mechanism for learning with sleep spindles. *Philosophical Transactions of the Royal Society B: Biological Sciences*, *375*(1799). https://doi.org/10.1098/rstb.2019.0230

Raju H, Tadi P. Neuroanatomy, Somatosensory Cortex. [Updated 2022 Nov 7]. In: StatPearls [Internet]. Treasure Island (FL): StatPearls Publishing; 2023 Jan-. Available from: https://www.ncbi.nlm.nih.gov/books/NBK555915/

Rayan, A., Agarwal, A., Samanta, A., Severijnen, E., van der Meij, J., & Genzel, L. (2022). Sleep scoring in rodents: Criteria, automatic approaches and outstanding issues. *European Journal of Neuroscience*. https://doi.org/10.1111/ejn.15884

Reddy S, Reddy V, Sharma S. Physiology, Circadian Rhythm. [Updated 2023 May 1]. In: StatPearls [Internet]. Treasure Island (FL): StatPearls Publishing; 2023 Jan-. Available from: https://www.ncbi.nlm.nih.gov/books/NBK519507/

Schabus, M., Gruber, G., Parapatics, S., Sauter, C., Klosch, G., Anderer, P., Klimesch, W., Salety, B., & Zeitlhofer, J. (2004). Sleep spindles and their significance for declarative memory consolidation. *Sleep*, *27*(8), 1479–1485. https://doi.org/https://doi.org/10.1093/sleep/27.7.1479

Schröder, J. K., Abdel-Hafiz, L., Ali, A. A. H., Cousin, T. C., Hallenberger, J., Rodrigues Almeida, F., Anstötz, M., Lenz, M., Vlachos, A., von Gall, C., & Tundo-Lavalle, F. (2023). Effects of the Light/Dark Phase and

Constant Light on Spatial Working Memory and Spine Plasticity in the Mouse Hippocampus. *Cells*, *12*(13), 1758. https://doi.org/10.3390/cells12131758

Seibt, J., Richard, C. J., Sigl-Glöckner, J., Takahashi, N., Kaplan, D. I., Doron, G., De Limoges, D., Bocklisch, C., & Larkum, M. E. (2017). Cortical dendritic activity correlates with spindle-rich oscillations during sleep in rodents. *Nature Communications*, *8*(1). https://doi.org/10.1038/s41467-017-00735-w

Tudor, J. C., Davis, E. J., Peixoto, L., Wimmer, M. E., Van Tilborg, E., Park, A. J., Poplawski, S. G., Chung, C. W., Havekes, R., Huang, J., Gatti, E., Pierre, P., & Abel, T. (2016). Sleep deprivation impairs memory by attenuating mTORC1-dependent protein synthesis. *Science Signaling*, *9*(425). https://doi.org/10.1126/scisignal.aad4949

Xia, Z., & Storm, D. (2017). Role of circadian rhythm and REM sleep for memory consolidation. *Neuroscience Research*, *118*, 13–20. https://doi.org/10.1016/j.neures.2017.04.011

Yamazaki, R., Toda, H., Libourel, P. A., Hayashi, Y., Vogt, K. E., & Sakurai, T. (2020). Evolutionary Origin of Distinct NREM and REM Sleep. *Frontiers in Psychology*, *11*. https://doi.org/10.3389/fpsyg.2020.567618

8. Supplementary materials

8.1 Objects and set-up NORT

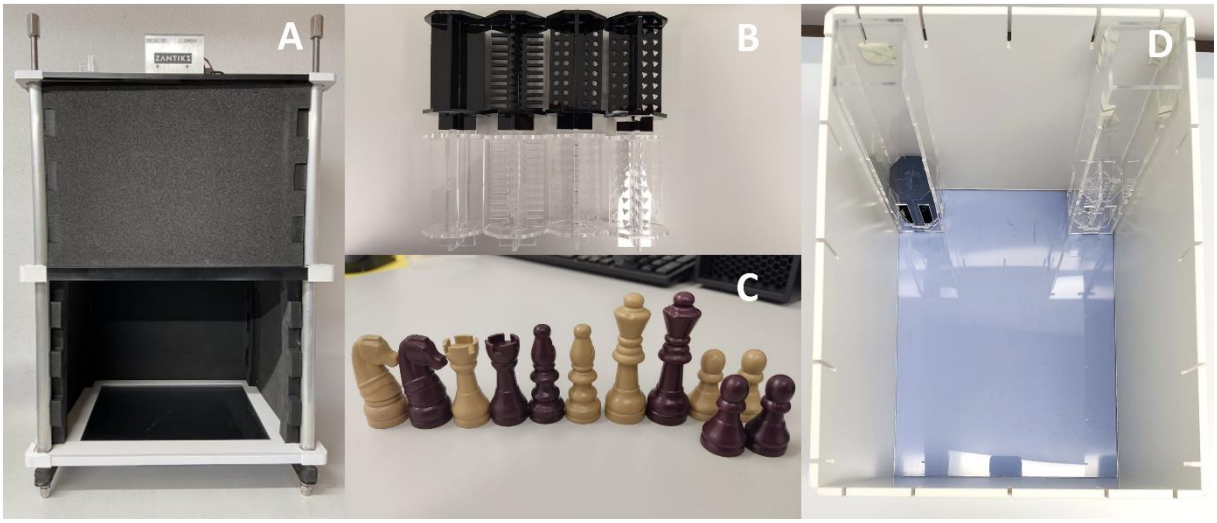

Figure 8: Configuration of the novel object recognition paradigm

The configuration of the novel object recognition paradigm is shown. Pictures depict the Zantiks LT unit (A), object configurations for different structures (B), object configurations for chess pieces (C) and the arena including two objects located in the acrylic towers (D).

8.2 Pilot study to determine appropriate antibody dilutions

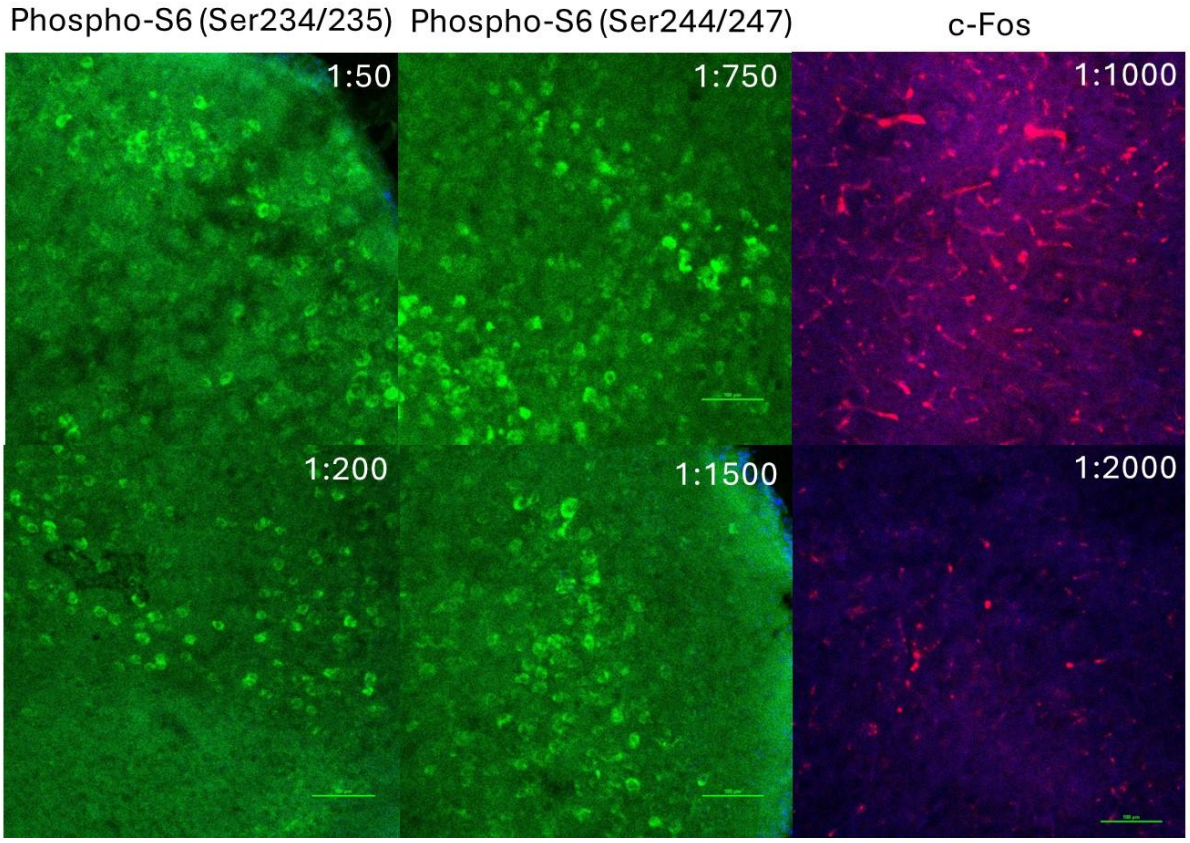

Figure 9: Images of Phospho-S6 and c-Fos antibody staining.

Images taken using the confocal microscope indicate staining for Phospho-S6 (Ser234/235) (left panel), Phospho-S6 (Ser244/247) (middle panel), and c-Fos (right panel). For each antibody, two dilutions are shown. The dilutions are as follows.
Phospho-S6 (Ser234/235): 1:50, 1:200,
Phospho-S6 (ser244/247): 1:750, 1:1500,
c-Fos: 1:1000, 1:2000.

8.3 Supplementary preference and discrimination tests

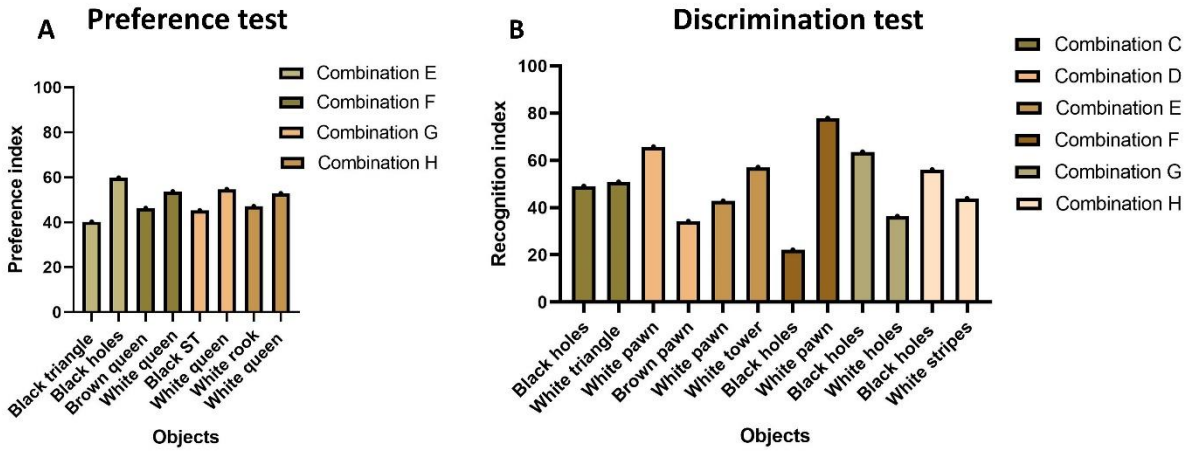

Figure 10: Supplementary pilot studies per object and combination for object selection.
Preference indices are shown for object combinations E (light green), F (dark green), G (beige) and H (brown) in the left panel. Recognition indices are shown for object combinations C (green), D (beige), E (brown), F (dark brown), G (light green) and H (wheat colour). The indices are plotted against the objects. Data are shown as mean + standard error of the mean (SEM) (n = 1). Pilot studies were executed for one animal per object combination. Object combinations in Fig. 3 were pursued during further experiments.